Journal of Thermal Analysis and Calorimetry, Vol. 73 (2003) 105–118

THERMAL ANALYSIS OF BLACK POWDER

R. Turcotte[*], *R. C. Fouchard, A.-M. Turcotte and D. E. G. Jones*

Canadian Explosives Research Laboratory, Natural Resources Canada, 555 Booth St., Ottawa, Ontario K1A 0G1, Canada

(Received March 3, 2003)

Abstract

While there is abundant literature describing the factors affecting the performance and the mechanical sensitivity of black powder, only a few papers are devoted to its thermal properties. Previous work indicated that no exothermic reactions were observed below 300°C in an inert gas environment. In the present work a variety of thermal techniques (DSC, TG, simultaneous TG-DTA-FTIR-MS, ARC, HFC) has been used to study the thermal decomposition of black powder. Exothermic reactions were observed at temperatures as low as 230 and 140°C in inert and oxidizing atmospheres, respectively. The latter exothermic reaction is due to sulfur oxidation.

Keywords: ARC, black powder, DSC, FTIR, HFC, mass spectrometry, TG, TG-DTA, thermal decomposition

Introduction

Black powder is the most ancient explosive known and the first documented energetic material. It has been used for over 800 years [1] and is still extensively used in the fireworks and pyrotechnic industries and for historical weapons. Black powder is a mixture of potassium nitrate, sulfur and charcoal. While the standard composition typically contains 75% potassium nitrate, 10% sulfur, and 15% charcoal, many variations have been used in order to obtain specific properties [2]. Although the combustion properties of black powder have been extensively studied [3, 4], much less information is available on its thermal behavior during the early stage of reaction. This low-temperature chemistry is important in determining the thermal hazards and the long-term stability of the material.

Perhaps the most comprehensive study on the early chemical processes occurring in the decomposition of black powder was that of Blackwood and Bowden [5]. They studied its thermal decomposition, below its ignition temperature, by monitoring the rate of gas evolution as a function of temperature. Chemical analysis of the gaseous and condensed products was also carried out in the same work. Their essen-

---

[*] Author for correspondence: E-mail: riturcot@nrcan.gc.ca

1388–6150/2003/ $ 20.00

Akadémiai Kiadó, Budapest
Kluwer Academic Publishers, Dordrecht

tial conclusions were that the initial reaction was between molten sulfur and the oxhydrocarbons (OHC) present in the charcoal, starting at about 150°C, but that the main reaction responsible for run-away was the oxidation of charcoal by KNO_3.

Campbell and Weingarten [6] carried out a thermal analysis study of black powder and its constituents using an in-house DTA apparatus with sample sizes up to 2 g. In these measurements, the DTA curves of black powder were characterized by a broad endotherm between approximately 95 and 200°C, followed by an exothermic pre-ignition reaction starting around 250°C and ignition taking place at about 300°C. They also carried out TG experiments on the same materials and measured ignition delay times using the method of Henkin and McGill [7]. In these experiments, virtually all the mass loss was observed in a single and extremely rapid step around 250°C. Their data support a reaction between S and KNO_3 as the pre-ignition reaction.

More recently, Brown and Rugunanan [9] have performed simultaneous TG-DTA studies on black powder in nitrogen while Hussain and Rees [8] published the results of DSC and TG/DTG experiments. In both cases, binary mixtures of its constituents were also investigated. Their main conclusions were that, while no reaction is observed between sulfur and charcoal, the energy release from the oxidation of organic material might enable the reaction of S and KNO_3 below the melting point of KNO_3. While they regarded the latter as the ‘pre-ignition’ reaction, the strongly exothermic oxidation of the charcoal by KNO_3, which takes place between 350 and 550°C, is the one that appeared to propagate the combustion of black powder.

This paper presents results obtained using a variety of thermal techniques: differential scanning calorimetry (DSC), thermogravimetry (TG), simultaneous thermogravimetric and differential thermal analysis (TG-DTA) combined with gaseous product detection by Fourier transform infrared spectrometry (FTIR) and mass spectrometry (MS), accelerating rate calorimetry (ARC), and heat flux calorimetry (HFC). By using this combination of methods to generate complementary information, it is possible to obtain a much more complete understanding of the system being studied than would be possible with a single experimental technique. Some results obtained at the early stage of this study have already been presented [10].

Experimental

DSC

A TA Instruments 2910 DSC was used for these measurements. The instrument was purged at a rate of 50 cm^3 min^{-1} with dry and oxygen-free nitrogen. A heating rate of 5°C min^{-1} was employed. Open aluminum pans and sealed glass ampoules were used for the measurements. In the first case, the sample size was approximately 5 mg while in the second case it was 0.5 mg. Temperature and heat flow calibrations were performed prior to the experiments according to ASTM procedures [11].

TG

A TA Instruments 2950 TG instrument was used. In these experiments, approximately 5 mg of sample material was held in a platinum pan, in a flow of dry nitrogen (100 cm^3 min^{-1}, split 60:40 between the furnace and the balance). Again, a heating rate of 5°C min^{-1} was employed. The TG instrument was calibrated for mass and temperature. The standard reference mass used for mass calibration was checked against a Mettler M3 microbalance with a precision of ±1 μg. The temperature was calibrated using the ASTM Curie point magnetic procedure with SRM nickel [12].

Simultaneous TG-DTA-FTIR-MS

Simultaneous thermogravimetry - differential thermal analysis was carried out using a TA Instruments SDT 2960 instrument, with evolved gas analysis using a Bomem MB100 FTIR spectrometer and a Balzers Thermostar GS300 quadrupole mass spectrometer. The TG-DTA-FTIR-MS data were acquired simultaneously in the same run. For these experiments, approximately 5 mg of sample material was placed in an alumina pan. The DTA reference material consisted of about 5 mg of platinum foil. The sample and the reference were purged with a 50 cm^3 min^{-1} flow of dry air or helium. The temperature was ramped from ambient to 500°C at a rate of 5°C min^{-1}.

The FTIR interface consisted of a 5 mm i.d. Teflon tube and a Pyrex cell (10 cm long, 50 cm^3 internal volume) equipped with KBr windows. A quartz microfiber filter was placed at the FTIR inlet. The acquisition rate of the FTIR was 1 scan min^{-1} and the time delay from the SDT furnace outlet to the FTIR cell was about 10 s. Bomem Grams 32 software was utilized for data acquisition and analysis.

The mass spectrometer data were acquired using the Balzers Quadstar 422 software. The heated quartz capillary interface was placed near the sample pan, in the SDT furnace. Data were acquired using bar graph scan, programmed to acquired data from 1 to 120 amu (atomic mass unit) at a speed of 0.2 s amu^{-1}.

TG mass together with DTA baseline and temperature calibrations (indium and tin) were performed prior to the experiments.

It should be pointed out that, while chemical analysis of solid residues would have been useful to identify solid decomposition products, such work could not be performed in the present study.

ARC

The experiments were carried out using one of the ARCs available at the Canadian Explosives Research Laboratory (CERL). This ARC is an automated adiabatic calorimeter distributed by Arthur D. Little Inc. and is used for the purpose of assessing the thermal hazard potential of energetic materials [13]. Adiabatic conditions are maintained in this ARC provided that the rate of temperature increase does not exceed about 10°C min^{-1}. Experiments were carried out using standard CERL procedures already described in earlier publications [14–16].

For these experiments, samples of 0.2 to 2 g of black powder were placed in lightmass spherical titanium vessels and experiments were performed with the ARC manifold closed in order to maintain any pressure resulting from vaporization or decomposition of the sample. Experiments were conducted both in an inert atmosphere (Ar) and air.

For all experiments, the sample was heated quickly and equilibrated at the chosen initial temperature. It was then subjected to the standard ARC procedure of 'heat-wait-search'. In this study, the temperature of the system was raised in 5°C increments and the system was maintained adiabatic during the 'wait' period (30 min for dissipation of thermal transients) and the 'search' period (20 min looking for an exotherm). An exotherm was defined as a self-heating rate (R) greater than the pre-selected threshold value of 0.02°C min^{-1}. Since exotherms are not detected during the 'heat' or 'wait' modes, the 'true' value of the onset temperature for thermal run-away (T_0) is obtained by extrapolating to R=0. Whenever an exotherm is detected during the search mode, the heat-wait-search procedure is automatically interrupted, and the calorimeter tracks the time, temperature, rate (calculated) and pressure. Data collection was programmed to stop if the pressure exceeded a set value (usually 6.89 MPa or 1000 psia), or R exceeded a certain value (usually 5°C min^{-1}).

HFC

A Setaram C-80 heat flux calorimeter was used for these experiments. Modifications to this instrument with high-pressure manifold and cells have already been described in detail elsewhere [17]. Two experimental methods were employed. In the first one, samples of 0.1 to 1.0 g were loaded directly into the high-pressure cell. Dry air or argon could then be introduced to vary the nature and initial pressure of the initial atmosphere. In the second method, less than 0.1 g of sample material was sealed in a glass ampoule with an internal volume of approximately 0.7 cm^3. The gas contained within the ampoule was air, but helium was used to provide good thermal contact between the ampoule and the walls of the cell. The heating rate for these HFC experiments was either 0.1 or 0.3°C min^{-1}.

Table 1 Characteristics of black powder samples used in the present work

Sample number	Grade	Grain size/mm	Manufacturer
1	2FA	2.0–6.4	Goex, USA
2	2FA	2.0–6.4	Pernambuco, Brazil
3	3FA	1.5–2.5	Goex, USA
4	3FA	1.5–2.5	Pernambuco, Brazil
5	5FA	0.5–1.3	Goex, USA
6	5FA	0.5–1.3	Pernambuco, Brazil
7	5FA	0.5–1.3	Kemijiska Industrija, Slovenia
8	XF Meal	<0.2	Goex, USA

Materials

A number of different samples of black powder was used during the course of this work. Table 1 summarizes the data on their grades, grain sizes, and origin.

Results

DSC and TG

Figure 1 shows typical DSC (bottom) and TG (top) curves obtained for 5FA black powder, with a heating rate of 5°C min^{-1}. Rather than the single rapid mass loss step around 250°C observed by Campbell and Weingarten [6], the TG curve in inert gas environment (N_2) obtained in the present work shows two distinct mass loss steps. This is most probably due to the faster heating rate they were using (15°C min^{-1}). In the first step, occurring below 200°C, 10% of the mass is lost, which corresponds to the vaporization of sulfur. In this temperature range, the corresponding DSC curve (open Al pan) shows the rhombic to monoclinic sulfur phase transition at 108°C (1), the melting of sulfur at 116°C (2), and the KNO_3 rhombic to trigonal phase transition at 133°C (3). The second mass loss step occurs between 200 and 450°C. In the latter, approximately 33% of the mass is lost. In this temperature domain, the features of the open Al pan DSC curve are a gradual increase in exothermic heat flow starting around 200°C, a sharp endothermic peak indicating the melting point of KNO_3 (330°C, (4)), and a broad exothermic peak, between 350 and 450°C, corresponding to the oxidation of the charcoal by KNO_3.

TG experiments were also performed in air and the results are also shown in Fig. 1. Careful inspection of the two TG curves reveals that the second mass loss step in air took place at lower temperature than in nitrogen.

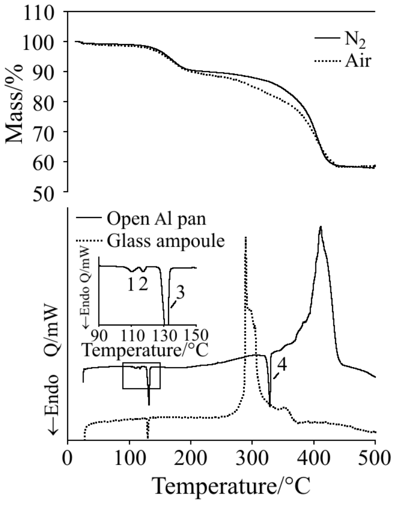

Fig. 1 Typical TG (top) and DSC (bottom) results for 5FA black powder (note that DSC baselines were shifted for clarity)

DSC experiments with 0.5 mg of black powder in a sealed glass micro-ampoule were also carried out and these results are compared to those obtained in an open Al pan in Fig. 1. It is seen that, while the KNO_3 phase transition is still observed, the onset of the charcoal/KNO_3 reaction occurs at a much lower temperature (285±3°C), so that the peak corresponding to the melting of KNO_3 has disappeared, masked by the complex exothermic structure.

Simultaneous TG-DTA-FTIR-MS

The results of a typical simultaneous TG-DTA run on 5FA black powder in an inert atmosphere (He), at a heating rate of 5°C min^{-1}, are shown in Fig. 2 (top). The TG curve is in close agreement with that of the previous section with 10% mass loss in the first step and about 33% mass loss in the second step. The DTA curve displays the same endotherms associated with melting and phase transitions for S and KNO_3 already seen in the DSC experiments. Additionally, the oxidation of charcoal by KNO_3 is observed to start at a slightly higher temperature than in the corresponding DSC experiment.

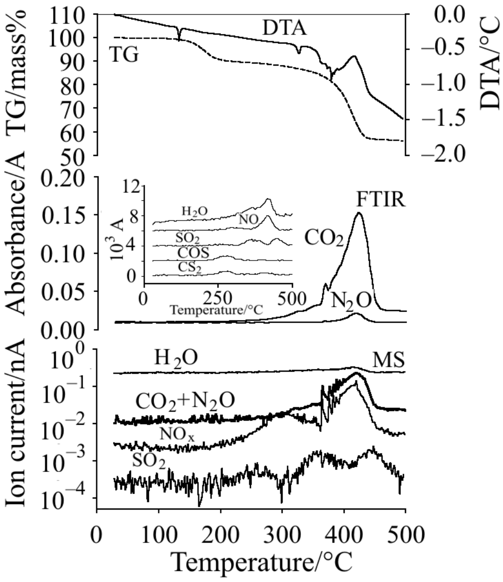

Fig. 2 Simultaneous TG-DTA (top), FTIR (center), and MS (bottom) results for 5FA black powder in helium (note that FTIR baselines have been shifted for clarity in the inset)

A number of products were observed in the gas phase. The FTIR data in Fig. 2 (center) are shown as absorbances, while the MS data (bottom) are displayed as ion currents. Although the FTIR and MS data are not calibrated for quantitative measurements, approximate relative concentrations for some of the gaseous species can be obtained using the scaling factors of Brill *et al.* [18]. The latter can be used to convert absorbance intensity of equal partial pressures of gases to concentrations relative to CO_2. The results of this conversion are shown in Table 2. It is clear that CO_2, NO and N_2O were the most abundant gaseous products observed. In helium, their evolution was observed to start around 200°C, at the beginning of the second mass loss step, and to increase sharply around 350°C. It is important to notice that no trace of H_2S could be detected in the present work. Traces of two sulfur compounds, COS and CS_2, were observed at temperatures below the melting point of KNO_3, while the evolution of water vapor and nitrogen oxides was observed to coincide with CO_2 production. Traces of SO_2 were also detected. In this case, two maxima were observed around 350°C, where the production of CO_2 starts to increase sharply, and around 450°C, close to completion of the second mass loss step.

Table 2 Relative concentration of some gaseous species observed by FTIR

Product	Frequency/ cm^{-1}	Scaling factor	Helium (50 cm^3 min^{-1})		Dry air (50 cm^3 min^{-1})	
			T_{max} */°C	C_{max} **	T_{max} */°C	C_{max} **
CO_2	2349	1.0	420	1.00	300 420	0.49 1.00
N_2O	2224	1.86	420	0.16	420	0.08
NO	1903	32.1	300 420	0.10 0.46	300 420	0.10 0.16
NO_2	1621	2.0	420	–	420	0.01

*Temperature at maximum of absorbance peak
**Relative concentration at maximum of absorbance peak

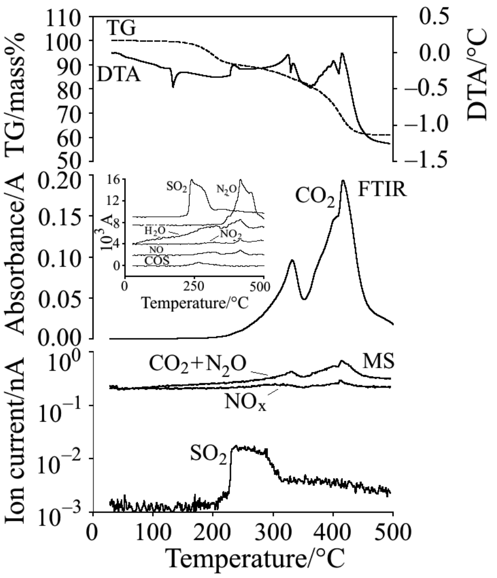

Fig. 3 Simultaneous TG-DTA (top), FTIR (center), and MS (bottom) results for 5FA black powder in air (note that FTIR baselines have been shifted for clarity in the inset)

Very significant differences were observed when the same experiment was carried out in air, as seen from Fig. 3. While the TG curve is quite similar, less mass loss was found to occur in the second step (28.7 % in air compared to 32.9% in helium). In addition to the usual endotherms corresponding to melting and phase changes of S and KNO_3, a new broad exotherm was observed around 230°C. As seen from the FTIR and MS data, this exotherm coincides with the appearance of SO_2 in the gas phase. Another broad exotherm, extending from 275 to 350°C and partially masking the KNO_3 melting endotherm, was also observed to coincide with a first peak in the CO_2 evolution. These features were not observed in the experiment under inert atmosphere. Only the second intense CO_2 peak in the 350 to 450°C range, corresponding to the oxidation of the charcoal by KNO_3, was observed in both cases. In the experiment performed in air, the latter peak coincides with trace amounts of N_2O, NO, NO_2 and H_2O. The relative concentrations of the first three species, computed using the scaling factors of Brill *et al.* [18], are also shown in Table 2.

ARC

Experiments on 5FA black powder using ARC were carried out both in ambient and elevated pressure atmospheres of argon and air. Typical results are shown in Fig. 4.

In argon at ambient initial pressure, several experiments were performed with sample masses from 0.2 to 2 g, using various initial temperatures (35, 100 and 200°C). No systematic dependence of T_0 upon these two variables was observed. It should be mentioned that when a 2 g sample was used, the run-away reaction was violent enough to explode the ARC sample vessel. Again, when argon at elevated initial pressure (1.4 MPa) was used, no significant difference in the value of T_0 was found. A sample mean of all the measurements performed under an inert atmosphere yielded the value of 225±14°C for T_0. In all cases, the Arrhenius plots of the exotherm data (Fig. 4, bottom) were found to be linear, except for the early stage of the exotherms. As for the onset temperature, the activation energies (E) obtained from linear fits to the ln(Rate) *vs.* $1/T$ data showed no systematic dependence on the various physical parameters mentioned above. A sample mean from all the linear fits yielded the value E=252±48 kJ mol^{-1}.

Several experiments were also performed with 0.5 g samples in air at ambient pressure and using various initial temperatures. Again no significant differences in T_0 and E values were observed and sample means of T_0=234±7°C and E=268±19 kJ mol^{-1} were obtained.

When experiments were carried out with 0.5 g samples in air at elevated initial pressure (1.4 MPa), a very different behavior was observed. The system was found to go into run-away at much lower temperature (T_0=141±5°C). Also, in this case, the Arrhenius plot was observed to be much more linear (Fig. 4, bottom) with a much higher activation energy (E=601±11 kJ mol^{-1}).

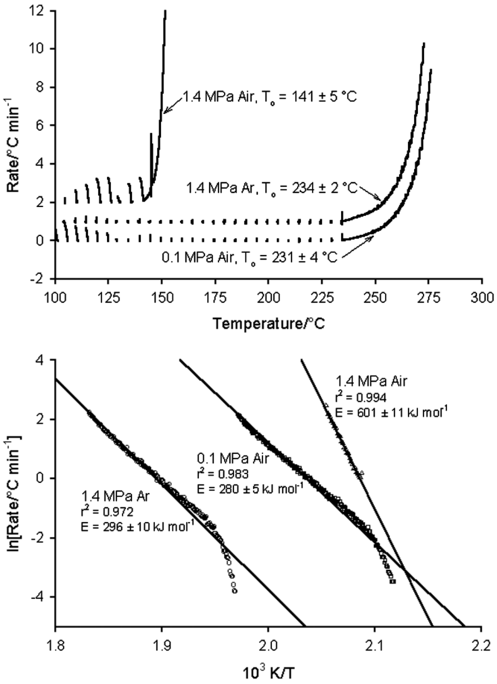

Fig. 4 Typical rate *vs*. temperature (top) and Arrhenius (bottom) plots from ARC experiments on 5FA black powder in argon and air (note that, for clarity, curves have been shifted along the vertical axis for the top graph and along the horizontal axis for the bottom graph)

HFC

Experiments using HFC were carried out under a variety of experimental conditions and on black powders of various grain sizes and origins. The results obtained for 5FA black powder in open cells and under an ambient pressure argon atmosphere are summarized in Fig. 5 (top). The same endothermic peaks observed below 200°C in the DSC experiments (phase transition of sulfur (1), melting of sulfur (2), and phase transition of KNO_3 (3)) are also seen here. Using a 0.1 g sample and a heating rate of 0.3°C min^{-1}, the exothermic reactions are observed at about 230°C. In order to obtain the full HFC curve, the heating rate was reduced from 0.3 to 0.1°C min^{-1}. In this case, it is seen that the position of the exothermic peak shifted to lower temperature and that the reaction started at about 210°C. These results also yielded a value of $\Delta H = -1.4$ kJ g^{-1}. In both cases the observed shift in the baseline is believed to result from the vaporization of sulfur. The sample size was also increased to 0.5 and to 1 g. In these cases, ignition was observed even in an inert gas environment. This behavior is also illustrated in Fig. 5 (top) for a 0.5 g sample. It is seen that, even with a heating rate of 0.3°C min^{-1}, the exothermic reaction is detected at an even lower temperature (190°C).

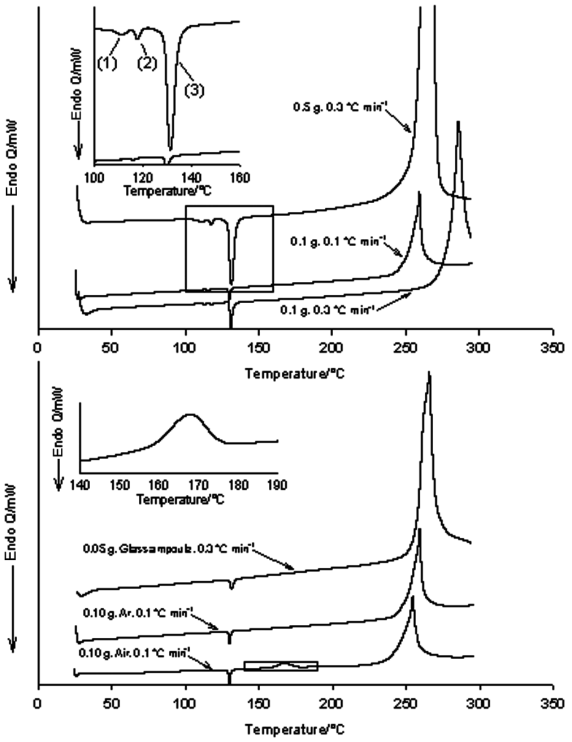

Fig. 5 HFC results in argon (top) and in various configurations (bottom) for 5FA black powder (note that baselines were shifted for clarity)

Samples were also loaded in sealed glass ampoules at ambient pressure of air. In these cases, the ampoule was introduced in the sample cell, which was then loaded with helium. In order to prevent rupture of the ampoule and thus contain the whole reaction in the latter, the sample size had to be decreased to 0.05 g. A typical result obtained with a heating rate of 0.3°C min^{-1} is compared to that described above for a 0.1 g sample in argon (0.1°C min^{-1}) in Fig. 5 (bottom). About twice the exothermic energy (in excess of 2.4 kJ g^{-1}) is observed under the confinement of the ampoule. Also, even though a faster heating rate was used with the ampoule, the exothermic reaction is observed at approximately the same temperature (230°C).

HFC experiments were also carried out with the sample loaded directly in the high pressure sample cell at ambient pressure of air. The results of an experiment using a sample size of 0.1 g and a heating rate of 0.1°C min^{-1} are also shown in Fig. 5 (bottom). Two observations can be made when these results are compared to those obtained under the same conditions in argon: (*i*) the exothermic reaction is observed at a slightly lower temperature in air (212°C in air *vs.* 230°C in argon), and (*ii*) a weak exothermic peak is observed between 150 and 180°C. While the latter is rather weak (99 J g^{-1}), it provides evidence of sulfur oxidation at low temperature even at ambient pressure of air.

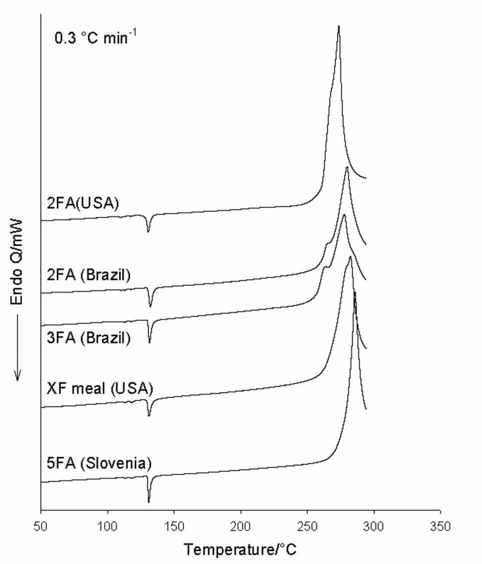

Fig. 6 HFC results in argon for black powders of various grain sizes and origins (note that baselines were shifted for clarity)

It is well known that the performance of black powder is affected by the particle size. In order to determine if the latter also has an effect on its thermal behavior, HFC studies were carried out on samples of various grain sizes and origins (Table 1). A sample size of 0.1 g and a heating rate of 0.3°C min^{-1} were used for these experiments. The results are compared in Fig. 6. It is seen that, while the peak temperatures are not a strong function of the particle size, the exothermic reactions for some larger grain size samples (2FA and 3FA from Brazil) are more complex as shown by the left shoulder in the corresponding main exotherms. It also appears that the origin of the sample plays an important role in the observed thermal behavior, as the two 2FA samples from different origin (USA and Brazil) display a very different shape for the main exotherm.

Discussion

The TG and DSC results for the open pan system reported here are similar to those of Brown and Rugunanan [9]. When the system is confined, as in the glass microampoules, it is seen that onset temperatures well under 300°C are observed. This is probably due to the fact that the reaction gases do not escape, and these gases accelerate the reaction. This confinement effect was also confirmed by the HFC experiments, in which much higher exothermic energy release was observed with sealed glass ampoules. The presence of air in the ampoule may also promote oxidation of organic material, which, in turn, may enable more sulfur oxidation by KNO_3 [8].

The simultaneous TG-DTA-FTIR-MS results in a helium atmosphere (Fig. 2) show that no gas evolution was detected in the first mass loss step (T<200°C). This may be due to the fact that the volatile organic species condense before reaching the FTIR cell. In contrast to the data obtained by Blackwood and Bowden [5], no H_2S production is observed in the early stage of decomposition. This is probably due to the fact that, in the present work, the system was constantly purged with helium or dry air while they were using a closed system. In the present case, the vaporized S would constantly be swept away while the volatile organic species might be condensing rapidly, leaving insufficient residence time for the formation of a detectable concentration of H_2S. This interpretation is consistent with earlier work reported [6, 8]. It also suggests that, if there were a contributing reaction between S and OHC, it would have to occur in the vapor phase rather than the molten state.

The formation of traces of COS and CS_2 early in the second mass loss step is probably occurring in the gas phase as both S and CO_2 are evolved at that stage. From Table 2, it is seen that CO_2, NO, and N_2O are the most important observed gaseous species. While CO_2 and N_2O have only one major peak with a maximum at 420°C, NO displays another peak with a maximum at about 300°C. This early NO production is consistent with the following reaction:

$$S+2KNO_3 \rightarrow K_2SO_4+2NO \tag{1}$$

The latter was first proposed by Campbell and Weingarten [6] as the pre-ignition reaction.

Various other reactions have been proposed for the oxidation of charcoal by KNO_3, which is responsible for propagation [6, 19]. Earlier observations [8, 19] report K_2SO_4 and K_2CO_3 as the most abundant solid products from the combustion of black powder and CO_2, CO, and N_2 as the major gaseous products from the oxidation of C, taking place between 350 and 550°C. However, the present work clearly identifies CO_2, NO and N_2O as the major gaseous species evolved in this temperature range when the reaction occurs in helium. While NO production at this stage has also been observed by Blackwood and Bowden [5], the production of N_2O may be explained by a contribution from the reaction:

$$2KNO_3+2C \rightarrow 2CO_2+K_2O+N_2O \tag{2}$$

When the same experiments were repeated in air, the mass loss obtained in the second step was found to be lower than in helium (28.7% compared to 32.9%). This can be explained by the formation of even more K_2SO_4 from the reaction

$$2KNO_3+SO_2 \rightarrow K_2SO_4+2NO_2 \tag{3}$$

as more SO_2 formation would result from the presence of O_2 in the gas phase. This is confirmed by the FTIR and MS data, both showing a sharp increase in SO_2 production at 228°C (Fig. 3). Also, when the experiment is carried out in air, two clear peaks are observed in the CO_2 evolution. The first one, at about 330°C, may be due to the oxidation of free carbon from the decomposition of the hydrocarbons contained in the charcoal also promoted by the presence of O_2 in the gas phase. The second peak would then be the result of oxidation of the charcoal by KNO_3.

The temperatures for the onset of run-away reactions in black powder obtained by ARC and HFC are much lower than those observed in DSC and DTA experiments. This is believed to be due to the larger sample sizes used in the former, which can lead to either an autocatalytic reaction or to quasi-adiabatic conditions in the central area of the samples. With 0.5 g samples, T_0 values as low as 190°C were observed in HFC experiments, even in an inert atmosphere. Also, direct oxidation of sulfur in the gas phase was observed at low temperature (160°C) in the HFC experiments in air at ambient pressure. This is consistent with the increased early SO_2 production noted above in the FTIR and MS observations. While no such low temperature exotherm could be observed in the corresponding ARC data, run-away is observed at a lower temperature (140°C) in the latter when an elevated initial air pressure was used. These observations may have important implications on the hazards of processing black powder, particularly under conditions where long residence times may occur with air intimately mixed with the powder, or under pressurized air atmosphere.

Significant variations in thermal behavior as a function of particle size were observed in the present work. It appears that larger particles may lead to lower T_0 values. However, the more complex exotherms displayed by samples with larger particle size may also result from the different origins of the samples. This may be caused by the use of different charcoal, for example. It is well known that variability in the characteristics of charcoal can cause significant differences in the thermal behavior of black powder [5, 20].

* * *

The authors would like to thank Hands Fireworks Inc. for providing some of the samples of black powder.

References

1 A. Marshall, 'Explosives – Their Manufacture, Properties, Tests and History', P. Blakiston's Son & Co., Philadelphia 1915.
2 J. P. Cundill, 'A Dictionary of Explosives', The Royal Engineers Institute, Chatham 1889.
3 R. A. Sasse, Proc. Int. Pyrotech. Seminar, 9 (1984) 47.
4 D. J. Wood, Proc. Int. Pyrotech. Seminar, 10 (1985) 71.
5 J. D. Blackwood and F. P. Bowden, Proc. Roy. Soc. A, 213 (1952) 285.
6 C. Campbell and G. Weingarten, Trans. Far. Soc., 55 (1959) 2221.
7 Henkin and McGill, Ind. Eng. Chem., 44 (1952) 1391.
8 G. Hussain and G. J. Rees, Propellants, Explosives, Pyrotechnics, 15 (1990) 43.
9 M. E. Brown and R. A. Rugunanan, Thermochim. Acta, 134 (1988) 413.
10 D. E. G. Jones, H. Feng and R. C. Fouchard, 4th Int. Sym. Fireworks, 1 (1998) 155.
11 ASTM E 967, ASTM E 968, American Society for Testing and Materials, West Conshohocken, PA, USA.
12 ASTM E 1582, American Society for Testing and Materials, West Conshohocken, PA, USA.

13 D. I. Townsend and J. C. Tou, Thermochim. Acta, 37 (1980) 1.
14 H. T. Feng, K. J. Mintz, R. A. Augsten and D. E. G. Jones, Thermochim. Acta, 311 (1998) 105.
15 D. E. G. Jones, H. T. Feng, R. A. Augsten and R. C. Fouchard J. Therm. Anal. Cal., 55 (1999) 9.
16 D. E. G. Jones, H. T. Feng, K. J. Mintz and R. A. Augsten, Thermochim. Acta, 331 (1999) 37.
17 D. E. G. Jones, P. Handa and H. Feng, J. Therm. Anal. Cal., 53 (1998) 3.
18 T. B. Brill, H. Arisawa, P. J. Brush, P. E. Congwer and G. K. Williams, J. Phys. Chem., 99 (1995) 1384.
19 I. Von Maltitz, J. Pyrotechnics, 14 (2001) 27.
20 G. Hussain and G. J. Rees, Propellants, Explosives, Pyrotechnics, 17 (1992) 1.